

Manuscript Number: ASR-D-10-00206R1

Title: Study of the seasonal ozone profile variations at European high latitudes

Article Type: ES

Keywords: Ozone, seasonal variability, lower stratosphere, tropopause based climatology, chemical and dynamical processes

Corresponding Author: Dr. Rolf Werner, Ph.D

Corresponding Author's Institution: STIL

First Author: Rolf Werner, PhD

Order of Authors: Rolf Werner, PhD; Kerstin Stebel, PhD; Hans Georg Hansen, PhD; Ulf-Peter Hoppe, Prof.; Michael Gausa, PhD; Rigel Kivi, PhD; Peter von der Gathen, PhD; Yvan Orsolini, PhD; Natalia Kilifarska, PhD

**Abstract:** The geographic area at high latitudes beyond the polar circle is characterized with long darkness during the winter (polar night) and with a long summertime insolation (polar day). Consequentially, the polar vortex is formed and the surrounding strong polar jet is characterized by a strong potential vorticity gradient representing a horizontal transport barrier. The ozone dynamics of the lower and middle stratosphere is controlled both by chemical destruction processes and transport processes.

To study the seasonal ozone variation at high latitudes, ozone vertical distributions are examined, collected from the Arctic Lidar Observatory for Middle Atmosphere Research (ALOMAR) (69.3°N, 16.0°E,) station at Andenes and from the stations at Sodankylä (67.4°N, 26.6°E) and at Ny-Ålesund (78.9°N, 11.9°E). The data sets cover the time period from 1994 until 2004. We find a second ozone maximum near 13 -15 km, between the tropopause and the absolute ozone maximum near 17- 20 km. The maximum is built up by the combination of air mass transport and chemical ozone destruction, mainly caused by the NO<sub>x</sub> catalytic cycle, which begins after the polar night and intensifies with the increasing day length. Formation of a troposphere inversion layer is observed. The inversion layer is thicker and reaches higher altitudes in winter rather than in summer. However, the temperature inversion during summer is stronger. The formation of an enhanced ozone number density is observed during the spring-summer period. The ozone is accumulated or becomes poor by synoptic weather patterns just above the tropopause from spring to summer. In seasonal average an ozone enhancement above the tropopause is obtained.

The stronger temperature inversion during the summer period inhibits the vertical stratosphere-troposphere exchange. The horizontal advection in the upper troposphere and lower stratosphere is enforced during summer. The combination of these mechanisms generates a layer with a very low ozone number density above the troposphere inversion layer subsisting from June/July until the late autumn.

Suggested Reviewers:



## Study of the seasonal ozone variations at European high latitudes

R. Werner<sup>a</sup>, K. Stebel<sup>b</sup>, H.G. Hansen<sup>c</sup>, U.-P. Hoppe<sup>d</sup>, M. Gausa<sup>e</sup>, R. Kivi<sup>f</sup>, P. von der Gathen<sup>g</sup>, Y. Orsolini<sup>b</sup>, and N. Kilifarska<sup>h</sup>

<sup>a</sup>Institute for Space and Solar-Terrestrial Research, Bulgarian Academy of Sciences, Stara Zagora Department, PO Box 73, 6000 Stara Zagora, Bulgaria

<sup>b</sup>Norwegian Institute for Air Research (NILU), PO Box 100, N-2027 Kjeller, Norway

<sup>c</sup>Norwegian Institute for Air Research (NILU), The Polar Environmental Centre, Polarmiljøseneteret, N-9296 Tromsø, Norway

<sup>d</sup>Norwegian Defence Research Establishment (FFI), PO Box 25, N-2027, Kjeller, Norway

<sup>e</sup>Andoya Rocket Range, ALOMAR, Andenes PO Box 54, N-8483 Norway

<sup>f</sup>Arctic Research Centre, Finnish Meteorological Institute, Tahtelantie 62 99600 Sodankylä, Finland

<sup>g</sup>Alfred Wegener Institute for Polar and Marine Research (AWI), PO Box 600149, 14401 Potsdam, Germany

<sup>h</sup>Geophysical Institute, Bulgarian Academy of Sciences, Acad. G.Bonchev Str. Block 3, 1113 Sofia, Bulgaria

### Abstract

The geographic area at high latitudes beyond the polar circle is characterized with long darkness during the winter (polar night) and with a long summertime insolation (polar day). Consequentially, the polar vortex is formed and the surrounding strong polar jet is characterized by a strong potential vorticity gradient representing a horizontal transport barrier. The ozone dynamics of the lower and middle stratosphere is controlled both by chemical destruction processes and transport processes.

To study the seasonal ozone variation at high latitudes, ozone vertical distributions are examined, collected from the Arctic Lidar Observatory for Middle Atmosphere Research (ALOMAR) (69.3°N, 16.0°E,) station at Andenes and from the stations at Sodankylä (67.4°N, 26.6°E) and at Ny-Ålesund (78.9°N, 11.9°E). The data sets cover the time period from 1994 until 2004. We find a second ozone maximum near 13 -15 km, between the tropopause and the absolute ozone maximum near 17- 20 km. The maximum is built up by the combination of air mass transport and chemical ozone destruction, mainly caused by the NO<sub>x</sub> catalytic cycle, which begins after the polar night and intensifies with the increasing day length. Formation of a troposphere inversion layer is observed. The inversion layer is thicker and reaches higher altitudes in winter rather than in summer. However, the temperature inversion during summer is stronger. The formation of an enhanced ozone number density is observed during the spring-summer period. The ozone is accumulated or becomes poor by synoptic weather patterns just above the tropopause from spring to summer. In seasonal average an ozone enhancement above the tropopause is obtained.

The stronger temperature inversion during the summer period inhibits the vertical stratosphere-troposphere exchange. The horizontal advection in the upper troposphere and lower stratosphere is enforced during summer. The combination of these mechanisms generates a layer with a very low ozone number density above the troposphere inversion layer subsisting from June/July until the late autumn.

### 1. Introduction

The ozone dynamical and chemical processes during the late fall until the late spring at high latitudes at both hemispheres is related to the polar vortex. It is established by the radiatively cooled air in the lower and middle stratosphere during the long time of absence of solar light (polar winter). Consequently, the polar vortex is formed and the surrounding strong polar jet is characterized by a strong potential vorticity gradient representing a horizontal transport barrier. During the summer time insolation photochemical processes begin in the stratosphere.

The main features of the variations in the ozone profiles are related to the so called laminae. This means ozone layers with enhanced ozone concentration (positive laminae) or with reduced ozone concentration (negative laminae). Some authors denote with laminae only ozone extrema in the lowest stratosphere. The secondary ozone maxima are very strong laminae structures with ozone concentrations of the order of the magnitude of the mid-stratospheric ozone concentration maximum (Lemoine, 2004). The difference between the ozone laminae structures and the ozone secondary maximum is not large. Laminae structures occur very often in the late winter and early spring in the vicinity of the polar vortex and are associated with filament vortex structures, which are formed by different processes (see Krizan and Lastovicka, 2005 and citations herein). Hwang et al. (2007) have found secondary ozone peaks over the Korean Peninsula during the winter and spring, generally formed by stratosphere-to-troposphere transport. At middle latitudes, the laminae can be caused by differential advection due to the vertical shear associated with the subtropical eastward jet and the stationary Rossby wave embedded therein (Tomikawa et al. 2002). Negative laminae structures are generated by intrusions of ozone-poor tropical air into higher latitudes, see e.g., Manney et al. (2000). Lower ozone density in the lowermost stratosphere typically indicates that the air is of more tropical origin, while high density indicates air of more polar origin. Particularly at middle latitude, gravity waves undulate ozone profiles as shown e.g. by Reid et al. (1998) and by Pierce and Grant (1998). An ozone excess over northwest Europe was already confined to the lower stratosphere in the earlier work from Mantis et al. (1981).

Kivi et al. (2007) were studied the interannual and long-term variations in the ozone profiles over the Arctic from 1989 to 2003. They found a mean secondary ozone maximum between the tropopause and the 150 hPa altitude during May and August. However, other details were not submitted. Melo et al. (2008) have found an enhanced ozone layer at about 12 km in the average for the period during late August to September 1998, 2000, 2002 and 2004 with changing frequency of occurrence over Saskatchewan, Canada (52° N, 107° W). It was noted that these features appear to coincide with the temperature inversion layer, however, no systematic studies to prove this statement were done.

The concept of the temperature inversion layer was worked out by Birner et al. (2002). They have revealed a very strong inversion in the mean vertical temperature gradient and consequently a very sharp tropopause on average for two midlatitude radio sonde stations in Southern Germany. Using data from the USA radio sonde stations Birner (2006) has shown that the tropospheric inversion layer exists on average in the extratropics (about 30°N - 70°N).

## 2. Data used and data processing

To study the ozone variations at European high latitudes ozone profiles were used, obtained by soundings at the high latitude stations Ny-Ålesund (78.9°N, 11.9°E) and Sodankylä (67.4°N, 26.6°E) and ozone profiles resulting from ozone lidar measurements from the Arctic Lidar Observatory for Middle Atmosphere Research (ALOMAR) (69.3°N, 16.0°E) station at Andenes. The geopotential height, temperature, pressure, ozone partial pressure, horizontal wind direction and speed and the relative humidity were measured. The ozone partial pressure was determined by the Electrochemical Concentration Cells (ECC) of ozone sondes. The lidar measurements allow obtaining the temperature, ozone density, air density and the potential temperature depending on the altitude. The main goal of the ozone observations by sondes at high latitudes is the investigation of the Arctic ozone losses during wintertime and early spring and the connected physical and chemical processes (von der Gathen et al. 1995 and Rex et al. 2004). Therefore, the frequency of the winter-spring soundings is greater than the provided soundings during the summer and autumn period. During winter-spring some soundings were provided per week and during the summer and autumn the soundings were reduced to approximately one per week. The profile number varied from 40 up to 90 per year and per each station, performing the ozone soundings (at Ny-Ålesund and Sodankylä). The lidar observations at ALOMAR were not performed on a regular basis. These observations were carried out during measurement campaigns. For example, the atmospheric soundings by rocket experiments were supported by lidar measurements.

The original profile data were sampled from 1Hz to 0.1 Hz containing significant fluctuations, which were reduced by applying a threshold filter. The profile data were interpolated over an equidistant altitude grid with discrete steps of 100 meters.

## 3. Tropopause based climatology

To establish the relation of the ozone density variation with the temperature inversion layer at the tropopause, here we follow the concept of the tropopause-based climatology developed by Birner et al. (2002). The tropopause height  $z_{TP}$  was calculated for every temperature profile using the definition of the World Meteorological Organization (WMO), 1986, where the tropopause is defined as the lowest level at which the rate of temperature decrease with the height (the temperature lapse rate) drops down to  $2 \text{ K km}^{-1}$  or less and the lapse rate averaged between this level and any level within the next 2 km does not exceed  $2 \text{ K km}^{-1}$  (see Holton et al. 1995). By shifting the altitude  $z$  to  $z - z_{TP}$  every profile (of the temperature or of the ozone density) is related to the tropopause height. The vertical coordinate is readjusted by the time-averaged altitude of

the tropopause  $\overline{z_{TP}}$ :

$$z' = z - \overline{z_{TP}} + \overline{z_{TP}} \quad (1)$$

The averaging is performed over the entire time interval, in our case the time period from 1994 until 2004. The important step is the

determination of the time averaged meteorological quantity  $x(t, z)$  by  $\overline{x(t, z)}$ , where the overbar denotes the time average. The presentation of the mean meteorological quantities in the manner described above is the so-called tropopause-based climatology (TB climatology), where the characteristics related to the tropopause are preserved. (For details, see Birner et al. 2002 and Birner, 2006). By interpolation of the ozone profiles related to  $z'$ , ozone altitude-time distributions for every year and station were constructed.

## 4. Results and discussion

Distributions of the concerned meteorological quantity were constructed as a function of the altitude and time for every year and station. To get smoother distributions the profiles were interpolated over time. The successive soundings reached different altitudes. If the profile ended at an altitude lower than the subsequent profile, the interpolation was carried out with the first subsequent profile, which reached the corresponding altitude. In the case when the time difference was larger than two weeks, no interpolation was performed to avoid side effects. All distributions were constructed for the time period of one year beginning in December of the previous year until November, which allowed the determination of seasonal means, beginning with the winter: December, January and February (DJF), spring: March, April and May (MAM), summer: June, July and August (JJA) and ending with the autumn: September, October and November (SON).

Fig. 1 shows the resulting ozone number density for year 2001/2002 obtained at ALOMAR and Sodankylä. In the overlapping time period both distributions were very similar because both stations probed approximately the same ozone volume. Therefore, only data from the Sodankylä and Ny-Ålesund ozone soundings will be involved in further studies.

An example of the temperature distribution for 2000 in TB-climatology from the Ny-Ålesund soundings is shown in Fig. 2a. The winter 1999/2000 was one of the coldest winters of the examined time period with very low temperatures in the middle stratosphere during the whole period from December until the middle of March. During the winter time Ny Ålesund was very often located below the polar vortex, which developed in the beginning of the polar night by radiative cooling of the air mass over the pole (Grewe, 2006). The density of the air mass increased with the decrease of the temperature. The descending heavy air mass was replaced by an air mass from the south. The diabatic vertical downward motion indicated a downward vertical advection of the chemical atmospheric constituents through the isentropic surfaces. The temperature distribution in Fig. 2a illustrates that during the polar winter the cold air mass probably descends slowly down to altitudes where the downward motion stops. The temperature inside the white contour is below 195K and signifies the possibility of polar stratospheric clouds formation. In Fig. 2b presents the plotted distribution of the temperature gradient of the temperature distribution, shown in Fig. 2a. To determine the temperature gradient and to obtain a smooth distribution, every temperature profile was smoothed. However, the profile was averaged only below the tropopause and, afterwards, above it. In this way the general profile of the temperature gradient around the tropopause was preserved. The yearly means were averaged over the seasonal means, which were calculated by averaging the monthly means. These stepwise calculations of the means balanced the different frequencies of the measured profiles during the year. Fig. 2b shows that the temperature gradient is changing very sharply at the tropopause and a temperature inversion layer (TIL) just above the tropopause is evident.

The measured temperature and pressure profiles allow to estimate the potential temperature  $\theta$  :

$$\theta = T (p_0/p)^\kappa, \quad (2)$$

where  $p_0$  is the surface pressure, taken to be 1000 hPa and  $\kappa$  is the ratio of the thermal capacity by constant volume and pressure,  $\kappa = c_v/c_p$  which is approximately 0.286 for dry air. The squared Brunt Väisälä frequency, which is a measure of the static stability, was calculated by the help of the potential temperature

$$N_B^2 = (g/\theta) (\delta\theta / \delta z). \quad (3)$$

A high static stability is generated as a consequence of the sharp change of the temperature gradient at the tropopause as illustrated in Fig. 3. The figure shows the static stability calculated for the same observations as in Fig. 2.

The seasonal profiles and yearly means in TB-climatology are valid only between the adjusted altitudes from approximately 4 km up to 30 km. The lower limit is a result of the adjustment of the profiles to the mean tropopause height. The upper limit is determined by the different altitudes reached by the ozone sondes.

The seasonal static stability was very high during the summer and autumn and restricted the vertical transport.

An example of the Sodankylä ozone distribution for the same time period in the standard surface related climatology is shown in Fig. 4. The tropopause height is outlined by a white line. As usual, the maximum mean ozone number density was observed during the winter and the lowest - during the autumn. The differences of the seasonal means characterize the net ozone production or loss between the successive seasons. With the beginning of the polar day, the processes of catalytic chemical ozone destruction are brought into action. Just above the tropopause, strong ozone variations are outlined, which is in agreement with the findings of Narayana Rao et al. (2004). In particular, the ozone number density changes over the whole year are well underlined in Fig. 4b., where the deviations of the ozone number density from the yearly means at every altitude are shown. These ozone density variations are due mainly to passage of low or high pressure systems. As an example, two ozone number density profiles observed at Sodankylä are shown (Fig. 5). The profiles from 5 July represents a secondary ozone maximum above the tropopause during the tropopause low period. The profile from 19 July is selected from the subsequent period characterized by a high tropopause, observed through temperature measurements. From 16 July until 19 July a stable low pressure system is located over the Scandinavian Peninsula, associated with some fronts. The inversion layer between 800 and 700 hPa is related to a front crossing Sodankylä, which is located in the warm sector of the depression. Warm air is transported from the south due to the warm conveyor belt along the cold front. The low pressure system is very strong and reaches the tropopause region. Using the Hysplit model, backward trajectories (<http://www.ready.noaa.gov/ready/open/hysplit4.html>) were calculated for the pressure level of 200 hPa just above the tropopause where very low ozone mixing ratio was observed (Fig. 6). A comparison of the determined backward trajectories with the ozone mixing ratio at the same pressure level (200 hPa), calculated by ERA-40 daily data ([http://data.ecmwf.int/data/d/era40\\_daily/](http://data.ecmwf.int/data/d/era40_daily/)) suggested that the low ozone content above the tropopause at altitudes between 11 km and 14 km on 19 July was generated by long-range horizontal transport of poor ozone air mass from the Northern Mediterranean to Northern Scandinavia. This is in a good agreement with the expected air mass transport from the 200 hPa level geopotential map (not shown here). It displays a strong low geopotential, centred over the Baltic Sea with a strong ridge at its eastern side, reaching Northern Scandinavia. The backward trajectories are approximately along the geopotential isolines and describe a circle centred in the low geopotential. The tropopause comes up to an altitude of 11.3 km. On 5 of July the tropopause height was approximately at 8.8 km.

The southern edge of the summer polar high pressure system was located over Sodankylä. The calculated backward trajectories demonstrated an air mass transport from the west together with the polar high pressure system and ozone rich air.

Consequently, the total ozone column over Sodankylä was larger on 5 July than on 19 July, as expected from the ozone profiles (Fig. 5) and as was found by satellite ozone measurements (e.g. TOMS Earth probe instrument Sodankylä overpass data, 329 DU and 285 DU, accordingly)

Mean seasonal profiles of the temperature, the static stability and the ozone number density were calculated for the whole time period from 1994 until 2004 for the Ny-Ålesund and the Sodankylä station (Fig. 7). A strong temperature inversion layer was found for the profiles of both stations, but the inversion at Ny-Ålesund (6.5 K) was stronger than at Sodankylä (5.5 K). The lower boundary of the TIL is the tropopause and as its upper limit in agreement with Bell and Geller (2008) we use the lower inflexion point of the static stability profile above the static jump at the tropopause. The TIL thickness is larger in the winter than in the summer. Both assertions, the stronger inversion at higher latitude and the bigger inversion during winter correspond with the results of Birner (2006). The mean spring ozone number density profiles are distinguished by a bulk at the winter TIL. As mentioned above, the ozone number density decrease during summer and autumn is caused by the catalytic chemical destruction of stratospheric ozone mainly driven by the  $HO_x$ ,  $XO_x$  (where X stands for halogen) and  $NO_x$  cycles (see Solomon, 1999). Fahey et al. (2000) have investigated the ozone destruction and production rates in the Arctic stratosphere and have pointed out the predominant role of  $NO_x$  and  $HO_x$  catalytic cycles at altitudes between 18 km and 20 km. Below 18 km, the  $HO_x$  cycle dominates the  $O_3$  destruction (Osterman et al. 1997).

The summer ozone number density profiles show a second maximum in the summer TIL just above the tropopause. As a second maximum we understand a simple local maximum in the averaged seasonal or yearly profile means. As noted above, this maximum is built up by the chemical destruction of ozone above the TIL and by horizontal transport processes. Vertical transport into the TIL during summer is strongly restricted by the high temperature inversion. A bulk of ozone is found in the mean spring profiles above the tropopause. An inflection point is assigned to the profile in the near of the upper TIL border.

In the spring-summer troposphere, ozone is produced as a result of photochemical reactions mainly by CO, CH<sub>4</sub>, and non-methane hydrocarbon. The maximum of the ozone mixing ratio in the layer around 15km has a maximum during summer, typically for photochemically produced ozone (Narayana Rao et al. 2004). In contrast to the tropics, where the produced ozone in the troposphere can be transported by vertical motion of air masses in the lower stratosphere, the tropospheric ozone can be transported in the lower stratosphere by troposphere-to-stratosphere exchange during summer. It is well documented that during summer the subtropical jet stream moves to the North. For the Sodankylä station, for example, the 320K isentrope of the potential temperature, which was calculated by equation (2), is located below the tropopause during the period from the end of April until the middle of September, which admits STE.

## 5. Conclusions

Distributions in TB-climatology of the temperature, ozone and the squared Brunt Väisälä frequency were constructed as a function of the altitude and time for every year and station. Seasonal mean profiles also in TB-climatology were calculated for these quantities. A secondary ozone maximum, located just above the tropopause at high latitude, for the studied time interval was observed every year from late spring and until to summer with varying amplitude. Stronger inversion was observed at higher latitude and during winter the inversion is bigger. It was shown that this second maximum is related to the TIL, with the lower boundary at the tropopause and as its upper limit the lower inflexion point of the static stability profile above the static jump at the tropopause.

A second ozone maximum, located just above the tropopause at high latitude is found every year in late spring and summer with varying amplitude. It is shown that the second ozone maximum is related to the temperature inversion layer. We demonstrate that the troposphere inversion layer at high latitudes is very stable, restricting the vertical transport. The inversion layer ozone is dynamically controlled by horizontal advection. Above the tropospheric inversion layer, the ozone is controlled rather more chemically and is destroyed catalytically. As a result of both processes, a second ozone maximum is built up.

## Acknowledgements

R. Werner was supported by the EU 6th FP within the ALOMAR eARI Project. The authors gratefully acknowledge the NOAA Air Resources Laboratory (ARL) for the provision of the HYSPLIT transport and dispersion model. We also thank to the ECMWF team for making available the ERA-40 data.

## References

- Bell, S. W., Geller, M. A. Tropopause inversion layer: Seasonal and latitudinal variations and representation in standard radiosonde data and global models. *J. Geophys. Res.* 113, D05109, 2008.
- Birner, T., Dörnbrack, A. and Schumann, U., "How sharp is the tropopause at midlatitudes", *Geophys. Res. Lett.* 29(14), 1700, 2002.
- Birner, T. Fine-scale structure of the extratropical tropopause region. *J. Geophys. Res.*, 111, D04104, 2006.
- Fahey, D. W., Gao, R.S., Del Negro, L.A., et al. Ozone destruction and production rates between spring and autumn in the Arctic stratosphere. *Geophys. Res. Lett.* 27, 2605-2608, 2000.
- Grewe, V. The origin of ozone. *Atmos. Chem. Phys.* 6, 1495-1511. 2006,
- Holton, J. R. Haynes, P. H., McIntyre M. E., et al. Stratosphere-troposphere exchange. *Reviews of. Geophys.* 33, 403-439, 1995.
- Hwang, S.-H., Kim, J. K., Cho, G.-R. Observation of secondary ozone peaks near the tropopause over the Korean Peninsula associated with stratosphere-troposphere exchange. *J. Geophys. Res.* 112, D13305, 2007.
- Kivi, R., Kyrö, E., Turunen, T., et al. Ozone sondes observations in the Arctic during 1989-2003: Ozone variability and trends in the lower stratosphere and free troposphere. *J. Geophys. Res.* 112, D08306, 2007.
- Krizan, P., Lastovicka, J. Trends in positive and negative laminae in the Northern Hemisphere. *J. Geophys. Res.* 110, D10107, 2005.
- Lemoina, R. Secondary ozone maxima in ozone profiles. *Atmos. Chem. Phys.* 4, 1085-1096, 2004.
- Manney, G. L., Michelsen, H. A., Irion, F. W. et al. Lamination and polar vortex development in fall from ATMOS long-lived trace gases observed during November 1994. *J. Geophys. Res.* 105, 29,023–29,038, 2000.
- Mantis, H.T., Repapis C.C, Zerefos, C.S. The summer maximum in total ozone over northwest Europe. *Pure Appl. Geophys.* 119, 213-230, 1981.
- Melo, S. M., Blatherwick, R., Davies, J., et al., Summertime stratospheric processes at northern mid-latitudes: comparison between MANTRA balloon measurements and the Canadian Middle Atmosphere Model. *Atmos. Chem. Phys.* 8, 2057-2071, 2008.
- Narayana Rao, T., Arvelius, J., Kirkwood, S., et al. Climatology of ozone in the troposphere and lower stratosphere over the European Arctic. *Adv. Space Res.* 34, 754-758, 2004.
- Osterman, G. B., Salawitch, R. J., Sen, B., et al. Balloon-borne measurements of stratospheric radicals and their precursors: Implications for the production and loss of ozone. *Geophys. Res. Lett.* 24, 1107-1110, 1997.
- Pierce, R. B., Grant W. B. Seasonal evolution of Rossby and gravity wave induced laminae in ozone data obtained at Wallops Island, Virginia. *Geophys. Res. Lett.* 25, 1859– 1862, 1998.
- Reid, S. J., et al. A study of ozone laminae using diabatic trajectories, contour advection and photochemical trajectory model simulations. *J. Atmos. Chem.* 30, 187– 207, 1998.
- Rex, M., Salawitch, R.J., von der Gathen, P., et al. Arctic ozone loss and climate change. *Geophys. Res. Lett.* 2004, 31, L04116, 2004.
- Tomikawa, Y., Sato, K., Kita, K., et al. Formation of an ozone laminae due to differential advection revealed by intensive observations. *J. Geophys. Res.* 107, 4092, 2002.
- Solomon, S., "Stratospheric Ozone Depletion: A Review of Concepts and History", *Rev. Geophysics*, 37, 275-316, 1999.
- von der Gathen, P., Rex, M., Harris, N. R. P., et al. Observational evidence for chemical ozone depletion over the Arctic in winter, 1991-92. *Nature*, 375, 131-134, 1995.

1  
2  
3  
4  
5  
6  
7  
8  
9  
10  
11  
12  
13  
14  
15  
16  
17  
18  
19  
20  
21  
22  
23  
24  
25  
26  
27  
28  
29  
30  
31  
32  
33  
34  
35  
36  
37  
38  
39  
40  
41  
42  
43  
44  
45  
46  
47  
48  
49  
50  
51  
52  
53  
54  
55  
56  
57  
58  
59  
60  
61  
62  
63  
64  
65

**Figure Captures:**

Fig.1. The reconstructed ozone distributions obtained from the ozone lidar measurements at ALOMAR and by the Sodankylä ozone sonde profiles during the overlapping measurement period from December 2000 until November 2001 are very similar because both stations studied approximately the same ozone volume.

Fig.2. The yearly temperature distribution and the seasonal and yearly means in TB-climatology for the observations at Ny Ålesund from December 1999 until November 2000 outlines very clearly the sharp temperature gradient change at the tropopause with a subsequent inversion layer above (a). The temperature inversion generates a sharp jump of the temperature gradient at the tropopause (b).

Fig.3. Static stability distribution derived from the observations at Ny Ålesund from December 1999 until November 2000 in TB-climatology. The temperature gradient jump generates high static stability at the tropopause, which restricts the vertical dynamics, particularly in summer.

Fig.4. a) Ozone number density distribution observed at Sodankylä from December 1999 until November 2000. b) The same as in a) but for the deviations from the yearly mean for every altitude.

Fig.5. Observed Sodankylä temperature profiles and ozone number density profiles during a low tropopause event (05.07.2000) and a high tropopause one (19.07.2000).

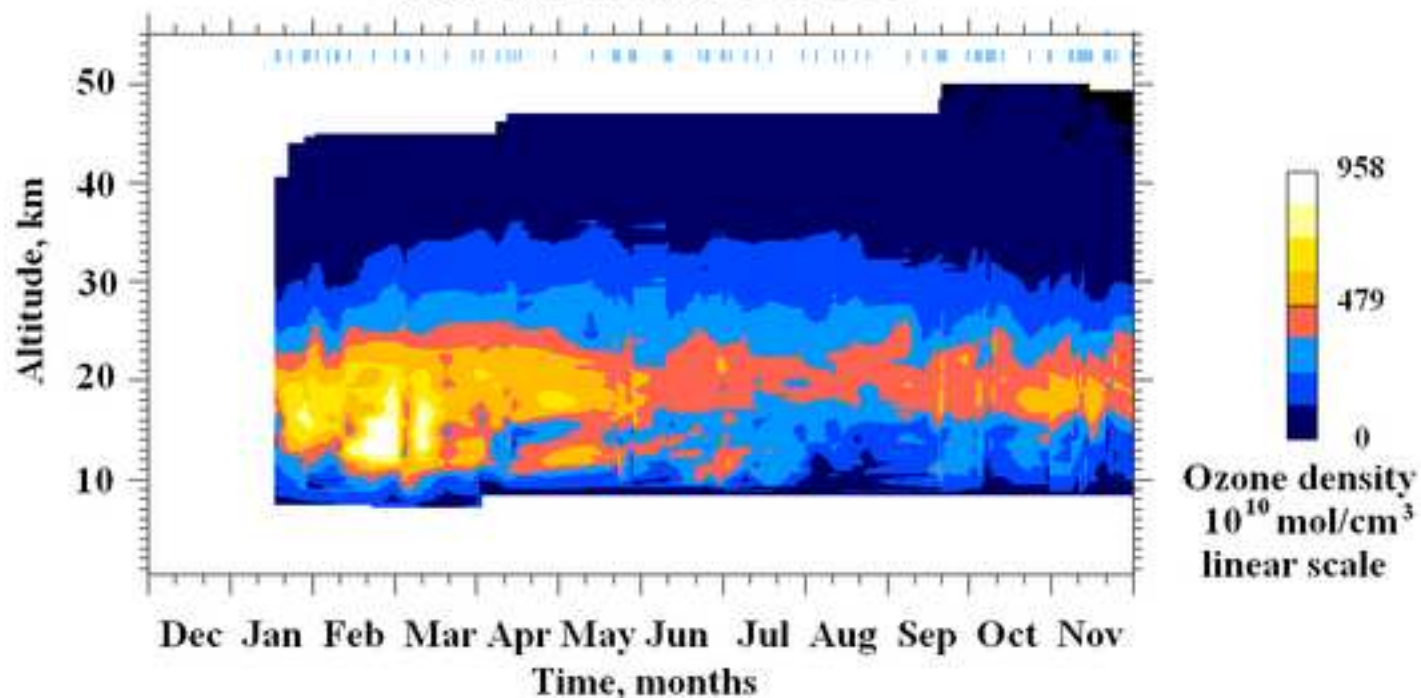
Fig.6. Ozone mixing ratio at the 200 hPa pressure level, based on the calculations of ERA-40 daily data. Backward trajectories calculated by the HYSPLIT model are drawn on the ozone mixing ratio map. The 4 trajectories for 19.07.2000 (upper panel) and 05.07.2000 (bottom panel) are calculated for 48 hours with a 12 hours step.

Fig.7. Mean seasonal profiles for the temperature (left panels), squared static stability (middle panels) and ozone number density (right panels) for the observations at Sodankylä (at top) and for Ny Ålesund (at bottom) for the time period from 1994 until 2004. The altitudes are related to the tropopause in TB-climatology. The horizontal lines represent approximately the bottom and the upper limit of the temperature inversion layer. The second ozone maximum, obtained in the seasonal means, is situated in the temperature inversion layer just above the tropopause and is related to the horizontal dynamics as a result of the large static stability of the inversion layer.

Figure1

[Click here to download high resolution image](#)

**ALOMAR ozone number density distribution  
from Dec. 2000 until Nov. 2001**



**Sodankylä ozone number density distribution  
from Dec. 2000 until Nov. 2001**

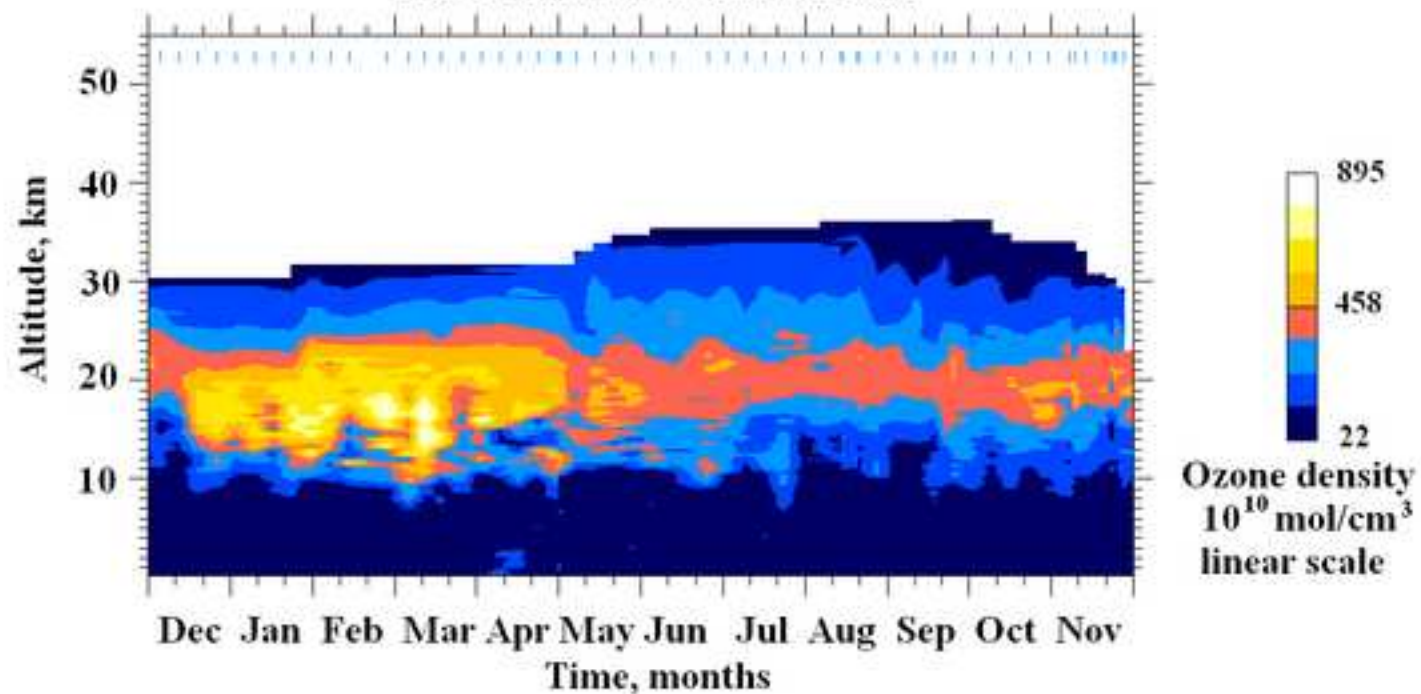




Figure2

[Click here to download high resolution image](#)

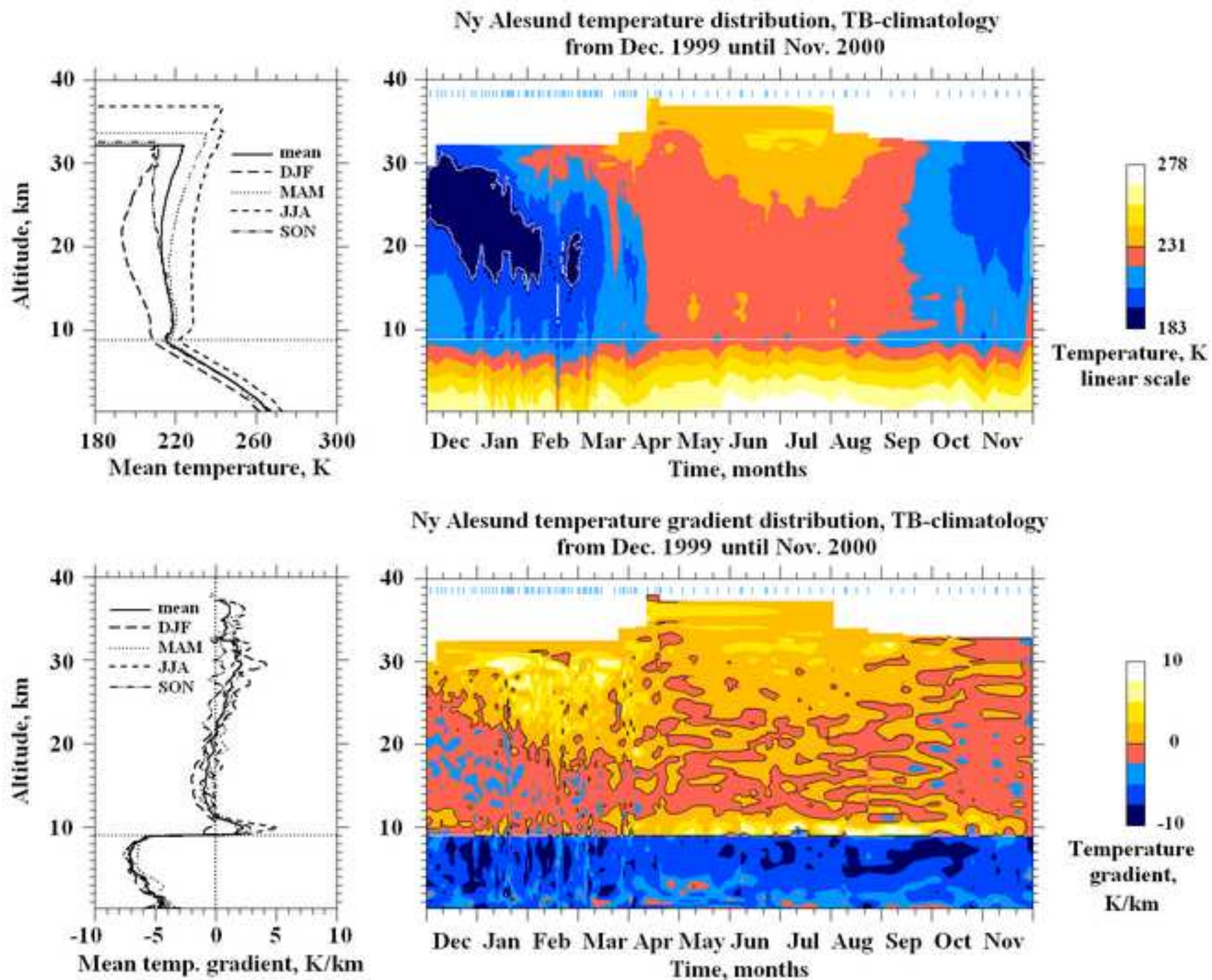


Figure3

[Click here to download high resolution image](#)

Ny Alesund stability distribution, TB-climatology  
from Dec. 1999 until Nov. 2000

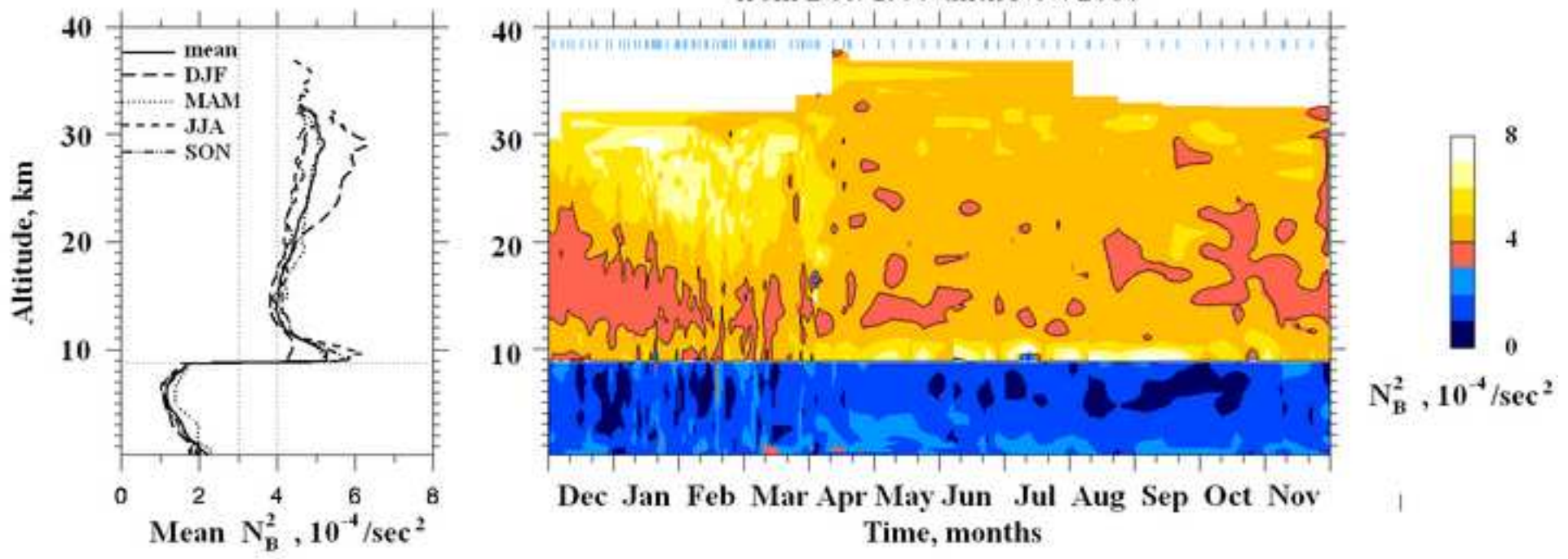


Figure4

[Click here to download high resolution image](#)

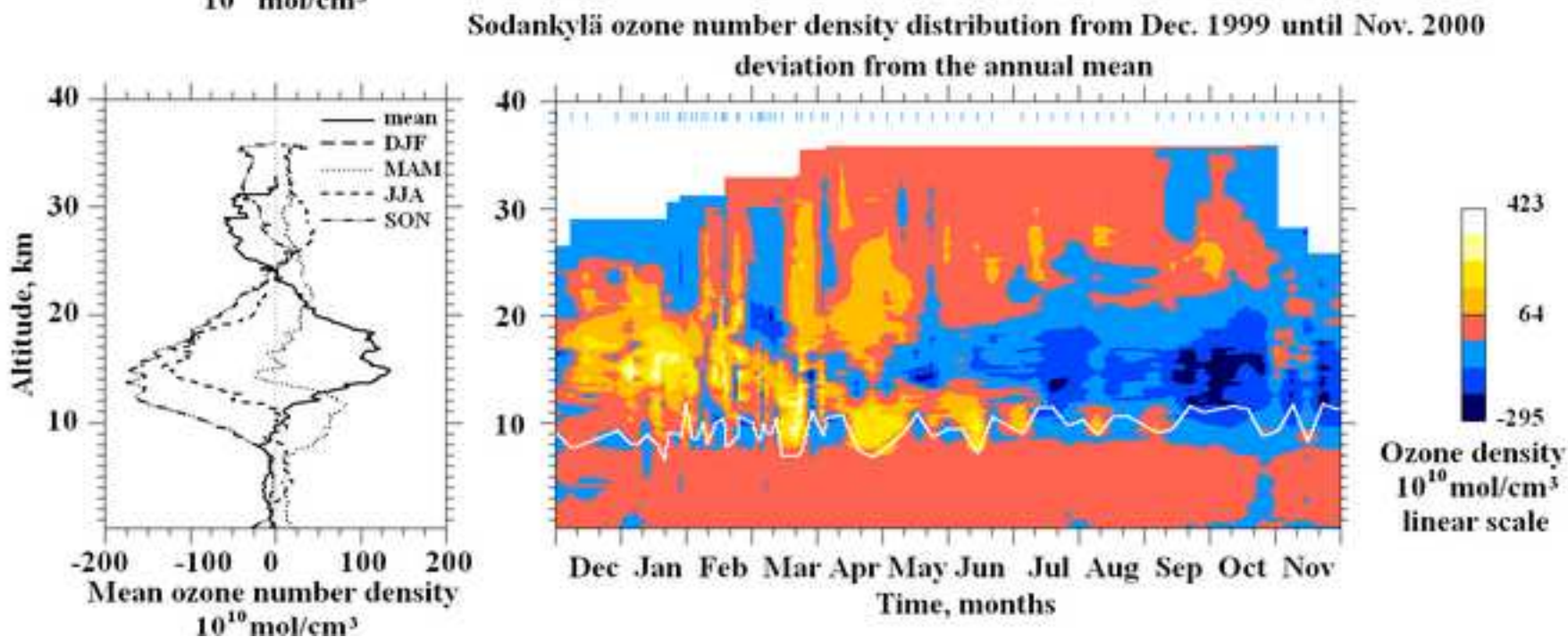
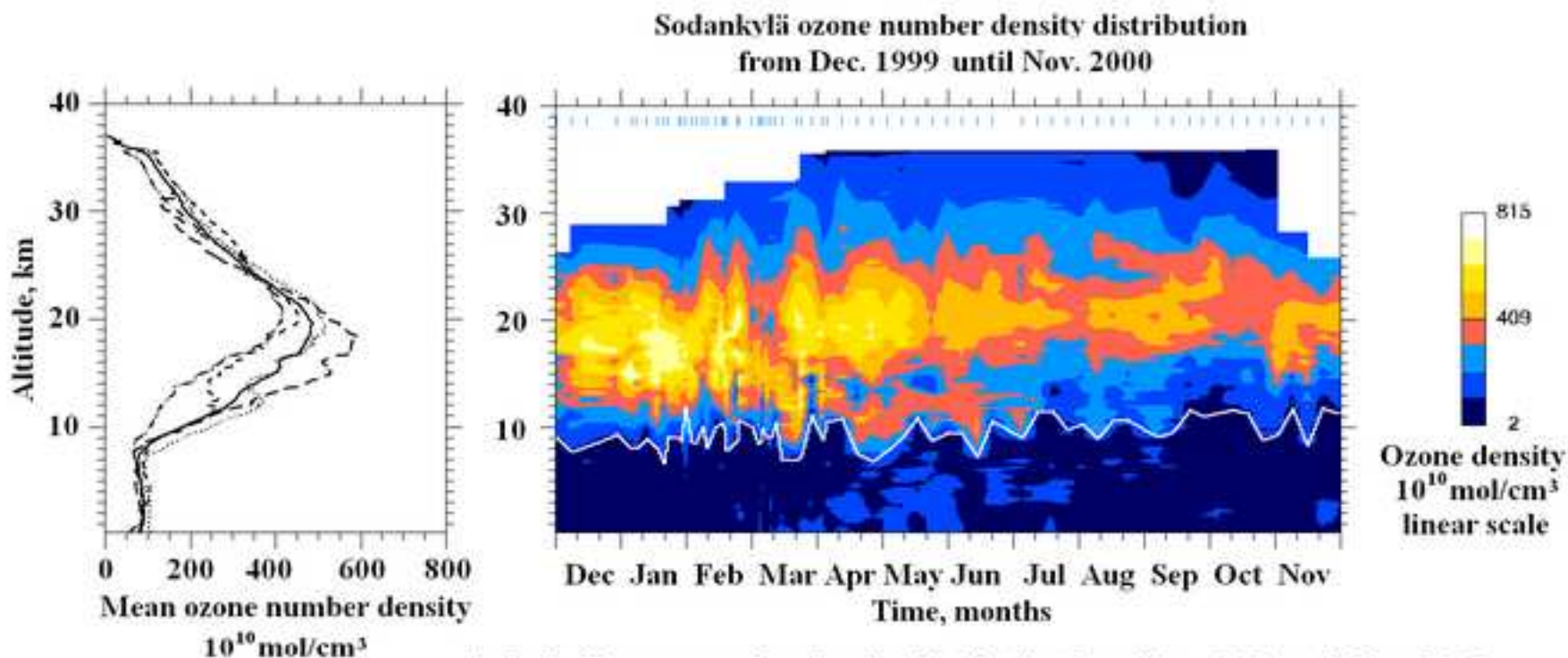


Figure5

[Click here to download high resolution image](#)

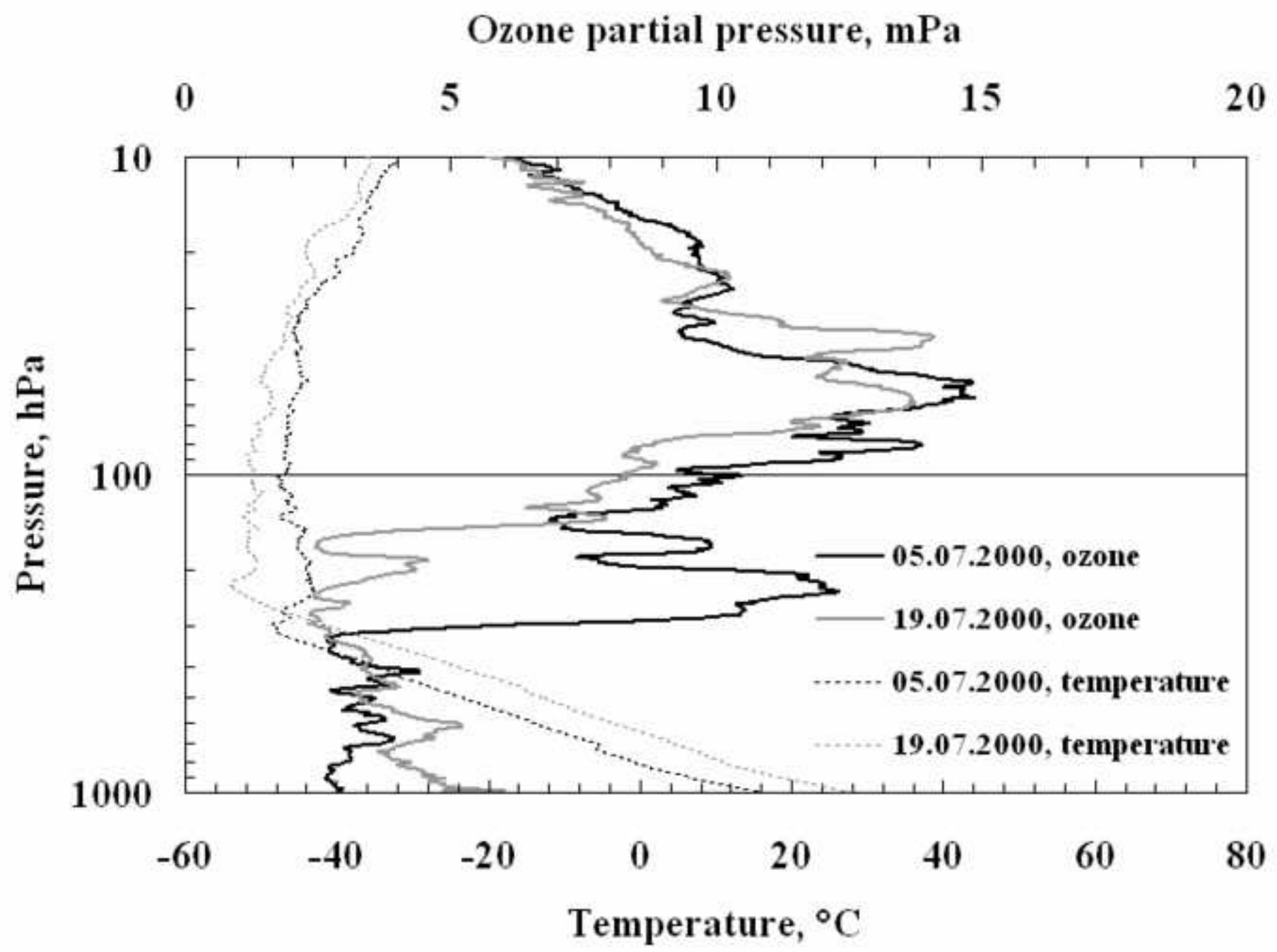


Figure6  
[Click here to download high resolution image](#)

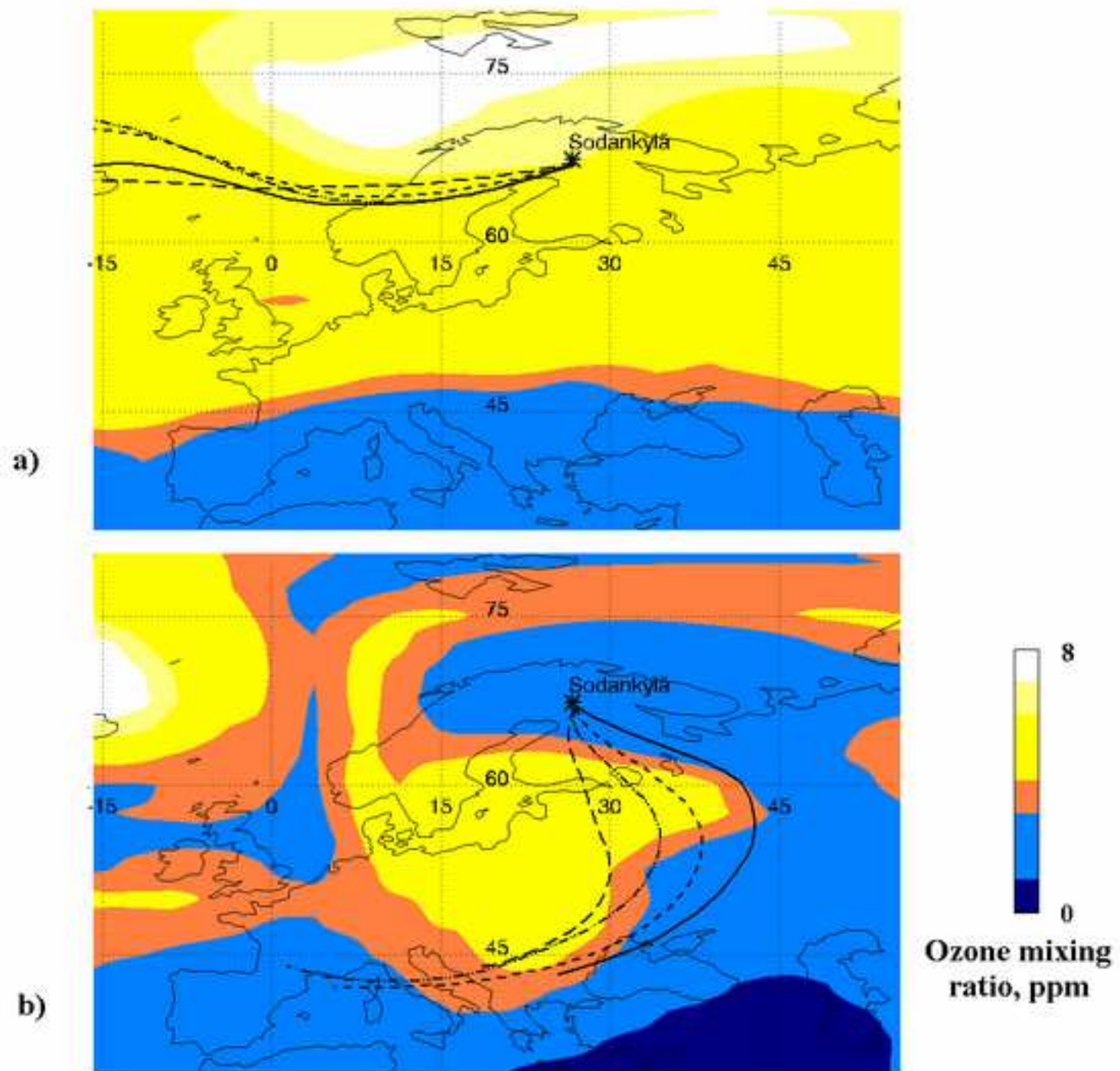


Figure7

[Click here to download high resolution image](#)

